Published in final edited form as:
Neuroimage. 2019 May 01; 191: 587–595. doi:10.1016/j.neuroimage.2019.02.023.

High-resolution metabolic mapping of gliomas via patch-based super-resolution magnetic resonance spectroscopic imaging at 7T

Gilbert Hangel[a,b], **Saurabh Jain**[c], **Elisabeth Springer**[a,b], **Eva Hečková**[a,b], **Bernhard Strasser**[d], **Michal Považan**[e,f], **Stephan Gruber**[a,b], **Georg Widhalm**[g], **Barbara Kiesel**[g], **Julia Furtner**[h], **Matthias Preusser**[i,j], **Thomas Roetzer**[k], **Siegfried Trattnig**[a,b], **Diana M. Sima**[c], **Dirk Smeets**[c], **Wolfgang Bogner**[a,b,*]

[a]High Field MR Centre, Department of Biomedical Imaging and Image-guided Therapy, Medical University of Vienna, Vienna, Austria

[b]Christian Doppler Laboratory for Clinical Molecular MR Imaging, Austria

[c]icometrix, R&D, Leuven, Belgium

[d]Athinoula A. Martinos Center for Biomedical Imaging, Department of Radiology, Massachusetts General Hospital, Harvard Medical School, Boston, MA, USA

[e]Russell H. Morgan Department of Radiology and Radiological Science, The Johns Hopkins University School of Medicine, Baltimore, MD, USA

[f]F. M. Kirby Research Center for Functional Brain Imaging, Kennedy Krieger Institute, Baltimore, MD, USA

[*]Corresponding author. Medical University of Vienna, Lazarettgasse 14, 1090, Wien, Vienna, Austria. wolfgang.bogner@meduniwien.ac.at (W. Bogner).

Conflicts of interest

M.Pr. personal DOIs

MP has received honoraria for lectures, consultation or advisory board participation from the following for-profit companies: Bristol-Myers Squibb, Novartis, Gerson Lehrman Group (GLG), CMC Contrast, GlaxoSmithKline, Mundipharma, Roche, Astra Zeneca, AbbVie, Lilly, Medahead, Daiichi Sankyo, Merck Sharp & Dome.

M.Pr. institutional DOIs

MP is responsible investigator for contracted research projects and clinical trials, for which research funding was paid to his institution by the following for-profit companies: Bristol-Myers Squibb, Böhringer-Ingelheim, GlaxoSmithKline, Merck Sharp & Dome and Roche.

Parts of the measurements in this manuscript were presented at the following conferences

Stephan Gruber, Gilbert Hangel, Eva Heckova, Bernhard Strasser; Michal Považan, Siegfried Trattnig, Wolfgang Bogner: *High resolution two and three dimensional fast magnetic resonance spectroscopic imaging of brain tumors at 7 T*; Radiological Society of North America, 103rd Scientific Assembly and Annual Meeting, 2017, Chicago, Illinois, United States of America.

Gilbert Hangel, Eva Heckova, Bernhard Strasser, Michal Považan, Stephan Gruber, Elisabeth Springer, Georg Widhalm, Matthias Preusser, Siegfried Trattnig, Wolfgang Bogner: *High resolution 7 T magnetic resonance spectroscopic imaging of glioma in the brain*; International Society for Magnetic Resonance in Medicine, 25th Annual Meeting, abstract number 309, 2017, Honolulu, Hawaii, United States of America.

Gilbert Hangel, Bernhard Strasser, Michal Považan, Stephan Gruber, Marek Chmelík, Georg Widhalm, Engelbert Knosp, Assunta Dal-Bianco, Fritz Leutmezer, Siegfried Trattnig, Wolfgang Bogner: *High resolution spectroscopic imaging with ultra short TE in patients with multiple sclerosis and brain tumors at 7 T*; International Society for Magnetic Resonance in Medicine, 23rd Annual Meeting, presentation number 0766, 2015, Toronto, Canada.

Early results of one patient were published in the following article (Fig. 8)

Stephan Gruber, Eva Hečková, Bernhard Strasser, Michal Považan, Gilbert Hangel, Lenka Minarikova, Marek Chmelík, Siegfried Trattnig, Wolfgang Bogner: *Mapping an Extended Neurochemical Profile at 3 and 7 T Using Accelerated High-Resolution Proton Magnetic Resonance Spectroscopic Imaging.* Invest Radiol 2017. https://doi.org/10.1097/RLI.0000000000000379.

Europe PMC Funders Author Manuscripts

[g]Department of Neurosurgery, Medical University of Vienna, Vienna, Austria

[h]Division of Neuroradiology and Musculoskeletal Radiology, Department of Biomedical Imaging and Image-guided Therapy, Medical University of Vienna, Vienna, Austria

[i]Department of Medicine I, Division of Oncology, Medical University of Vienna, Vienna, Austria

[j]Comprehensive Cancer Center Vienna, Medical University of Vienna, Vienna, Austria

[k]Institute of Neurology, Medical University of Vienna, Vienna, Austria

Europe PMC Funders Author Manuscripts

Abstract

Objectives—To demonstrate the feasibility of 7 T magnetic resonance spectroscopic imaging (MRSI), combined with patch-based super-resolution (PBSR) reconstruction, for high-resolution multi-metabolite mapping of gliomas.

Materials and methods—Ten patients with WHO grade II, III and IV gliomas (6/4, male/female; 45 ± 9 years old) were prospectively measured between 2014 and 2018 on a 7 T whole-body MR imager after routine 3 T magnetic resonance imaging (MRI) and positron emission tomography (PET). Free induction decay MRSI with a 64 × 64-matrix and a nominal voxel size of 3.4 × 3.4 × 8 mm^3 was acquired in six minutes, along with standard T1/T2-weighted MRI. Metabolic maps were obtained via spectral LCmodel processing and reconstructed to 0.9 × 0.9 × 8 mm^3 resolutions via PBSR.

Results—Metabolite maps obtained from combined 7 T MRSI and PBSR resolved the density of metabolic activity in the gliomas in unprecedented detail. Particularly in the more heterogeneous cases (e.g. post resection), metabolite maps enabled the identification of complex metabolic activities, which were in topographic agreement with PET enhancement.

Conclusions—PBSR-MRSI combines the benefits of ultra-high-field MR systems, cutting-edge MRSI, and advanced postprocessing to allow millimetric resolution molecular imaging of glioma tissue beyond standard methods. An ideal example is the accurate imaging of glutamine, which is a prime target of modern therapeutic approaches, made possible due to the higher spectral resolution of 7 T systems.

Keywords

MRSI; 7T; Patch-based super-resolution; Brain spectroscopy; Glioma; Glutamine

1 Introduction

In clinical practice, magnetic resonance imaging (MRI) is routinely applied for preoperative tumor characterization or regular investigation of gliomas in the postoperative follow-up period. However, MRI is frequently of limited diagnostic power for this purpose (Wang et al., 2016). Magnetic resonance spectroscopic imaging (MRSI) offers additional information through the mapping of the spatial distribution of multiple metabolites. Yet, clinical MRSI is often limited by low spatial resolution and rectangular selection boxes, and to the measurement of metabolite ratios, such as total choline (tCho) to total creatine (tCr) or tCho to total N-acetyl-aspartate (tNAA) ratios. Other compounds of interest, such as glutamine

(Gln), which was found to be more abundant in gliomas (Li et al., 2015) and a key piece in tumor metabolism, biosynthesis, and homeostasis (Altman et al., 2016) in general, cannot be quantified. Therefore, MRSI is mostly restricted to the distinction between low- and high-grade gliomas using average tCho/tCr- and tCho/tNAA-ratios derived from large volumes (Wang et al., 2016).

Higher spatial resolution and the quantification of more chemical compounds can be realized by free-induction-decay (FID) acquisition with ultra-short acquisition delay (Bogner et al., 2012; Henning et al., 2009). FID-MRSI eliminates signal loss due to T2-relaxation and J-coupling, improves spatial selection, reduces specific absorption rates (SAR), and accelerates data acquisition. These benefits make it robust in contrast to the limitations faced on ultra-high-field systems (Moser et al., 2012), which have, thus far, hindered the clinical application of high-resolution MRSI at 7 T (Li et al., 2015). At the same time, 7 T FID-MRSI offers new possibilities, such as the separation of neighboring resonances, such as glutamate (Glu) and Gln. FID-MRSI allows full-slice measurements without a selection box. Combined with efficient acceleration methods (Strasser et al., 2017), this enables high-resolution MRSI (i.e.,64 × 64 matrices and higher) in clinically feasible scan times (i.e.,~5–6min) (Hangel et al., 2016; Nassirpour et al., 2016).This is still insufficient for many clinical needs. Patch-based super-resolution (PBSR) uses prior knowledge from MR imaging to further reduce partial volume errors, thereby recovering spatial details from lower-resolution imaging, such as MRSI (Jain et al., 2017).

The aim of our proof-of-concept study was, therefore, to demonstrate the feasibility of 7 T-MRSI combined with PBSR reconstruction for high-resolution, multi-metabolite mapping of gliomas.

2 Materials and Methods

2.1 Subjects and hardware

The Departments of Neurosurgery and Oncology recruited patients between 2014 and 2018. The inclusion criteria were: glioma with non-significant contrast uptake prior to surgery (n = 7) or glioma with suspected recurrence (n = 3); no contraindications for MRI (e.g., claustrophobia, metal implants, pregnancy); routine MRI and positron emission tomography (PET); written, informed consent and institutional review board approval.

Ten data sets of patients with glioma (six male 40 ± 5 y, four female 52 ± 11 y) were prospectively acquired using a 7 T whole-body-MRI imager (Magnetom, Siemens Healthcare, Erlangen, Germany) after routine MRI examinations.

All tumors and their World Health Organization (WHO)-classification including isocitrate dehydrogenase- (IDH) and 1p/19q-status (Louis et al., 2016), are listed in Table 1. IDH-mutation status was assessed immuno-histochemically using an IDH1-R132H antibody (Dianova, #DIA-H09). 1p/19q-codeletion status was obtained by multiplex-dependent probe amplification using the SALSA MLPA P088 probemix (MRC Holland). Preliminary results of patient #7 were published previously (Gruber et al., 2017), but did not include data evaluation and PBSR as described below.

2.2 Measurement protocol

Clinical 3 T MRI included T1-weighted imaging (T1w) before and after contrast agent administration (Prohance), T2-weighted imaging (T2w), fluid-attenuated inversion recovery (FLAIR), and susceptibility-weighted imaging (SWI), as well as PET using F18-FET or C11-Methionine tracers.

7 T MRI included magnetization prepared rapid gradient echo (MPRAGE), magnetization prepared 2 rapid gradient echoes (MP2RAGE), SWI, FLAIR, and a B1+-mapping-based flip angle optimization (Table 2). All MRSI slices were positioned transversally and covered the suspected center of the glioma (i.e., maximum of hyperintense FLAIR regions).

2.3 MRSI sequence design

The high resolution FID-MRSI (Hangel et al., 2015; Strasser et al., 2017) sequence acquired a single slice with a 64 × 64-matrix and a field of view (FOV) of 220 × 220 × 8 mm^3 and full slice coverage (nominal voxel size 3.4 × 3.4 × 8 mm^3). Six-fold parallel imaging (PI)-acceleration using (Strasser et al., 2017) reduced the measurement time to six minutes. Further parameters were: TR 600 ms; acquisition delay 1.3 ms; 45° flip angle; 1024 readout points; 3000 Hz readout bandwidth; and water suppression enhanced through T_1 effects (WET) (Ogg et al., 1994) water suppression (Hangel et al., 2016, 2015; Strasser et al., 2017). Additionally, in patient #7, a three-fold accelerated (12 min) single-slice sequence was acquired, and in patient #3 a multi-slice MRSI sequence (Hangel et al., 2016) (15 min) was acquired, with the similar parameters as described above (Tbl.2).

2.4 Data processing

Offline MRSI processing was based on in-house-developed software using Matlab (R2013a, MathWorks, Natick, MA, USA), Bash (v4.2.25, Free Software Foundation, Boston, MA, USA), and MINC (MINC tools, v2.0, McConnell Brain Imaging Center, Montreal, QC, Canada) using: multichannel spectroscopic data combined by matching image calibration data (MUSICAL) coil combination (Strasser et al., 2013); parallel imaging reconstruction (Strasser et al., 2017); lipid signal removal using L1-regularization (Bilgic et al., 2013); and spatial Hamming filtering (resulting in a 2.7-times increased effective voxel size corresponding to an increase of in-plane voxel dimensions of 64%). Spectra were fitted with LCModel (v6.3–1, LCMODEL Inc, ONT, CA) between 1.8 and 4.2 ppm, with a basis-set of 17 metabolites (alanine, aspartate, Cr, gamma-aminobutyric acid, glucose, Glu, Gln, glutathione, glycerophosphocholine, Ins, lactate, NAA, N-acetyl-aspartyl glutamate, phosphocholine, phosphocreatine, scyllo-inositol, taurine) and a measured macromolecule background (Považan et al., 2018). Maps of tNAA, tCr, tCho, myo-Inositol (Ins), Glu, Gln and respective ratio maps to tCr and tNAA were created and masked as described under “data evaluation”.

T1w-, FLAIR-, T2w-, and CE-T1w-MRI data were skull-stripped and co-registered, and bias-field removal and tissue segmentation into grey matter (GM)/white matter (WM)/cerebrospinal fluid (CSF) were performed via FSL (FMRIB Software Library v5.0, Oxford, UK) prior to PBSR reconstruction. All gliomas were segmented by a neuroradiologist (E.S.) using only the co-registered MRI data. Finally, all metabolite (ratio) maps were four-fold up-

sampled using PBSR (Jain et al., 2017) from 3.4 × 3.4 × 8 to 0.9 × 0.9 × 8 mm^3 resolution using prior knowledge from T1w, FLAIR, and segmentations (GM, WM, CSF, lesion). The PBSR reconstruction used the tumor segmentation to drive the reconstruction using only the MRSI input within the tumor and only the MRI input outside of it.

2.4.1 Data evaluation—Spectral quality (i.e., signal-to-noise ratio (SNR) and full-width-at-half-maximum (FHWM) of tNAA) and fitting quality (i.e., Cramér–Rao lower bounds (CRLB) of all metabolites) were calculated voxel-wise. Low quality spectra (i.e., tNAA CRLB >20%, tCho + tCr + Ins CRLB>60%, and tNAA FWHM>0.15 ppm) were rejected during the generation of metabolite maps. Due to the small number and heterogeneity of gliomas, no statistical comparison was attempted. PBSR results were compared with the original maps and maps derived via standard linear interpolation. The added clinical value of high-resolution metabolite maps compared to the MRI and PET was qualitatively evaluated by two neuroradiologists (E.S., S.T.).

3 Results

3.1 General results

High-quality metabolic maps of tNAA, tCho, tCr, Glu, Gln, and Ins (Fig. 1) and spectra (Sup.1) were obtained in all MRSI scans. Some other metabolites in the basis-set (e.g., 2-hydroxyglutarate (2HG), glycine, lactate, glutathione) could not be quantified reliably (CRLBs >20%).

We noted a general increase of Gln levels in glioma, while Glu was generally reduced, except in case #7, a recurrent diffuse astrocytoma. A comprehensive overview of metabolite trends (Tbl.2) shows the expected decrease of tNAA and increase of tCho in all patients. The remaining metabolic alterations were heterogeneous within each tumor. We found decreased tCr in 5/9 (except #5, 6, 8, 9) and increased Ins in 6/9 patients (except #4, 7, 8).

3.2 PBSR-MRSI results

PBSR of metabolic maps improved the anatomic and pathologic details compared to the original or linear interpolation (Fig. 1). No visible artifacts were introduced. In more heterogeneous cases after resection or with recurrence and infiltration, PBSR-maps revealed locally different metabolic activities (especially Cho, Ins, Gln) within the glioma at high resolution, which was in excellent topographic agreement with PET (Fig. 2). In the only included grade IV glioma, increased Gln and tCho ratios corresponded to the contrast-enhanced T1w regions, while overall metabolic changes (e.g. tNAA and Ins drops) fit together well with the hyper-intense FLAIR regions (Fig. 3). In patient #9, the Gln ratio maps, indicate metabolic alterations beyond the FLAIR-hyper-intense regions also in tissue without significant contrast media uptake (Fig. 4). For patient #7, another case with a recurrent tumor, the metabolite maps show activity beyond/exceeding the contrast enhancement (Fig. 5). Multi-slice maps of patient #3 provided full coverage of the pathologic regions (Fig. 6) due to the increased field of view, allowing delineation of metabolic changes in the whole glioma and surroundings. In general, the PBSR ratio maps (e.g., patient #8, Sup.2) highlight metabolic alterations in gliomas in great detail.

4 Discussion

With this pilot study, we demonstrated fast, high-resolution mapping of six metabolites in glioma patients at 7 T. The resulting maps resolved spatial variations in tumor metabolisms in unprecedented detail. High-resolution metabolic imaging can define metabolic changes beyond morphological imaging.

4.1 Results in comparison to other research

To date, most MRS studies of gliomas were conducted at ≤3T and were restricted to NAA, Cho, Cr, and occasionally, Ins. Ratios of these were utilized for glioma grading (Boonzaier et al., 2017; Bulik et al., 2013; Caulo et al., 2014; Senft et al., 2009; Wang et al., 2016) in combination with other imaging modalities. Our results are in agreement with previous reports on decreased NAA, increased Cho, and mixed behavior in Cr concentrations (Bulik et al., 2013; Wang et al., 2016). Ratios to NAA perform better than those to Cr (Stadlbauer et al., 2007; Wang et al., 2016), possibly due to the variable behavior of Cr in different gliomas (Bulik et al., 2013), while NAA is consistently reduced. Elevated Cho/NAA ratios can reliably identify tumor infiltration outside contrast-enhancing regions (Boonzaier et al., 2017). Our results illustrate that higher spatial resolutions can better differentiate the density of active gliomas, which could improve applications like MRSI-guided biopsies (Cordova et al., 2016).

Biochemical research of tumor metabolism has shown the need to image changes of MRS-detectable substances, such as Glu, Gln, 2HG, glycine, and glutathione (Libby et al., 2018). Gln plays an important role in tumor metabolism, biosynthesis, and homeostasis, can be correlated to the expression of oncogenes, can suppress stress response in cells, and is an alternative carbon source instead of glucose in the tricarboxylic acid cycle (Altman et al., 2016). Further, Gln deprivation affects and can even kill tumor cells, making it a target for new therapies (Altman et al., 2016) such as glutaminase inhibitors. Thus, Gln imaging may be a critical addition to current imaging markers for glioma metabolism, even more so as Gln level changes can be expected in all gliomas (Altman et al., 2016; Li et al., 2015), while 2HG can only be measured in IDH-mutated gliomas.Compared to other 7 T-MRSI-approaches, our FID-MRSI sequence offers better spatial resolution, shorter measurement times, and full slice coverage (Hangel et al., 2016, 2015). To date, only one glioma study of 29 patients using 7 T-MRSI was published by (Li et al., 2015). It was limited to 1 cm^3 resolution (i.e., a 20 × 22 × 8 matrix in 11 min), while our approach with 0.095 cm^3 nominal resolution (i.e., 64 × 64 × 1 in 6min) is faster, despite the higher resolution. Their findings were similar to ours, with general increases of Ins, Gln, and Cho and decreases of Glu and NAA in glioma tissue. Admittedly, they were able to quantify increases in Gly and GSH concentrations reliably at this low resolution, which was not possible in our study.

4.2 Limitations

Our study is mainly limited by the small sample size that precludes in-depth statistical evaluation. This will be addressed in future studies. With larger patient populations, significant metabolic differences between tumor grades/types are expected (Li et al., 2015). Currently, we do not report absolute metabolite concentrations, but this is less critical in a

clinical setting and promising approaches are emerging (Moser et al., 2012). Due to the short TR, the MRSI sequence is affected by T1-weighting, which affects metabolite amplitudes and therefore the calculated metabolite ratios. Any interpretation of MRSI beyond the qualitative changes discussed in this work needs to account for this.T1-weighting should also be considered for any attempts of absolute quantification. Our FID-MRSI is currently limited to a maximum of four slices, but also full-brain 3D-MRSI has recently been demonstrated, and can be readily combined with PBSR for high-resolution, whole-brain metabolic mapping (Hingerl et al., 2018a, 2018b).

Our FID-MRSI sequence cannot reliably quantify 2HG due to the relatively low SNR of the accelerated MRSI sequence, and therefore, not directly assess the IDH-status. This requires other acquisition strategies like spectral editing (Andronesi et al., 2016). Another possible explanation for the lack of fittable 2HG that could be considered would be the misquantification of 2HG as Gln, but the distinct spectral separation between Gln and 2HG at 7 T (e.g. (Ganji et al., 2016), Fig. 1) as well as the lack of 2HG in the IDH-wildtype patient #10 indicate that 2HG is not erroneously fitted as Gln.

The PBSR algorithm is currently limited to segmentation of a single type of lesion and therefore cannot separate the glioma into compartments. Future implementations should use automated segmentation and separation of different lesion types.

FID-MRSI has recently been ported to clinical 3 T systems, but at a significant performance loss with regard to metabolite separation and measurement times (Gruber et al., 2017).

4.3 Conclusions

PBSR-MRSI combines the benefits of UHF systems, cutting-edge MRSI, and advanced postprocessing, thus allowing sub-millimeter, multi-metabolite mapping of glioma tissue and representing a relevant improvement over previous MRSI methods in gliomas. The resulting images are in excellent agreement with PET and previous MRS findings. As proof-of-concept, we were able to resolve different metabolite concentrations and therefore to differentiate metabolic activities within the gliomas, even beyond alterations visible on morphological imaging. This has a high potential for clinical use, as MRS was found to have the second-best diagnostic accuracy after T2w-MRI (Verburg et al., 2017), with already much lower resolutions or even just single-voxel MRS. High-resolution MRSI might allow profiling of metabolic density within a tumor and better differentiation of the characteristics of different gliom types. This can lead to improvements in glioma grading, personalized medicine (radiomics), therapy planning, and patient monitoring. An example would be the ability to define the best target area for tissue sampling during resections and biopsies in suspected gliomas. The ability to separate the metabolite Gln, for which tumor cells show an increased dependence (Altman et al., 2016), from Glu, and map it at a high resolution is another promising clinical application beyond current MRS applications. In contrast to 2HG, which is only detectable in gliomas with IDH-mutations, Gln levels appear to change in all gliomas (Altman et al., 2016; Li et al., 2015). With Gln being a progenitor of 2HG in the glioma metabolism and their relationship being under investigation (Seltzer et al., 2010), adding Gln mapping to the tools available for research might help our general understanding

Europe PMC Funders Author Manuscripts

of the glioma metabolism. Successful translation of FID-MRSI to whole-brain coverage and 3 T-systems could further improve the clinical impact.

The high-resolution imaging of multiple metabolites that are critically involved in tumor metabolism can improve the delineation of metabolic activity. In particular, the additional mapping of Gln opens new avenues to track glioma metabolism. This applies to the development of personalized medicine: It allows creating better tumor profiles to use for grading, resolving tissue structures for surgical planning and tumor sampling, post-operative monitoring, and adding critical information to radiomics.

Supplementary Material

Refer to Web version on PubMed Central for supplementary material.

Acknowledgements

This work received support from the Austrian Science Fund: KLI 646 and P 30701; the FFG Bridge Early Stage Grant #846505; and TRANSACT (EU-FP7-PEOPLE-2012-ITN-316679). The financial support by the Austrian Federal Ministry for Digital and Economic Affairs and the National Foundation for Research, Technology and Development is gratefully acknowledged.

Abbreviations

2HG	2-hydroxyglutarate
CE	contrast-enhanced
tCho	choline-containing compounds
CRLB	Cram'er-Rao lower bound
tCr	total creatine, creatine + phosphocreatine
CSF	cerebrospinal fluid
FID	free induction decay
FLAIR	fluid-attenuated inversion recovery
FOV	field of view
FWHM	full width at half maximum
Gln	glutamine
Glu	glutamate
GM	grey matter
IDH	isocitrate dehydrogenase
Ins	inositol
MPRAGE	magnetization prepared rapid gradient echo

Europe PMC Funders Author Manuscripts

MP2RAGE	magnetization-prepared 2 rapid acquisition gradient echoes
MRSI	magnetic resonance spectroscopic imaging
MUSICAL	multichannel spectroscopic data combined by matching image calibration data
tNAA	total N-acetyl-aspartate, N-acetyl-aspartate + N-acetyl-aspartyl glutamate
NAWM	normal-appearing white matter
PBSR	patch-based superresolution
PET	positron emission tomography
PI	parallel imaging
ROI	region of interest
SAR	specific absorption rate
Sl	slice
SNR	signal-to-noise ratio
SWI	susceptibility-weighted imaging
T1w	T1-weighted
T2w	T2-weighted
TE	echo time
TR	repetition time
WET	water suppression enhanced through T1 effects
WM	white matter

References

Altman BJ, Stine ZE, Dang CV. From Krebs to clinic: glutamine metabolism to cancer therapy. Nat Rev Canc. 2016; 16:619–634. DOI: 10.1038/nrc.2016.71

Andronesi OC, Loebel F, Bogner W, Marjanska M, Vander Heiden MG, Iafrate AJ, Dietrich J, Batchelor TT, Gerstner ER, Kaelin WG, Chi AS, et al. Treatment response assessment in IDH-mutant glioma patients by noninvasive 3D functional spectroscopic mapping of 2-hydroxyglutarate. Clin Cancer Res. 2016; 22:1632–1641. DOI: 10.1158/1078-0432.CCR-15-0656 [PubMed: 26534967]

Bilgic B, Gagoski B, Kok T, Adalsteinsson E. Lipid suppression in CSI with spatial priors and highly undersampled peripheral k-space. Magn Reson Med. 2013; 69:1501–1511. DOI: 10.1002/mrm.24399 [PubMed: 22807147]

Bogner W, Gruber S, Trattnig S, Chmelik M. High-resolution mapping of human brain metabolites by free induction decay 1H MRSI at 7 T. NMR Biomed. 2012; 25:873–882. DOI: 10.1002/nbm.1805 [PubMed: 22190245]

Boonzaier NR, Larkin TJ, Matys T, van der Hoorn A, Yan J-L, Price SJ. Multiparametric MR imaging of diffusion and perfusion in contrast-enhancing and nonenhancing components in patients with glioblastoma. Radiology. 2017; 284:180–190. DOI: 10.1148/radiol.2017160150 [PubMed: 28240563]

Bulik M, Jancalek R, Vanicek J, Skoch A, Mechl M. Potential of MR spectroscopy for assessment of glioma grading. Clin Neurol Neurosurg. 2013; 115:146–153. DOI: 10.1016/j.clineuro.2012.11.002 [PubMed: 23237636]

Caulo M, Panara V, Tortora D, Mattei PA, Briganti C, Pravatà E, Salice S, Cotroneo AR, Tartaro A. Data-driven grading of brain gliomas: a multiparametric MR imaging study. Radiology. 2014; 272:494–503. DOI: 10.1148/radiol.14132040 [PubMed: 24661247]

Cordova JS, Gurbani SS, Olson JJ, Liang Z, Cooper LAD, Shu H-KG, Schreibmann E, Neill SG, Hadjipanayis CG, Holder CA, Shim H. A systematic pipeline for the objective comparison of whole-brain spectroscopic MRI with histology in biopsy specimens from grade III glioma. Tomogr a J imaging Res. 2016; 2:106–116. DOI: 10.18383/j.tom.2016.00136

Ganji SK, An Z, Tiwari V, McNeil S, Pinho MC, Pan E, Mickey BE, Maher EA, Choi C. In vivo detection of 2-hydroxyglutarate in brain tumors by optimized point-resolved spectroscopy (PRESS) at 7T. Magn Reson Med. 2016; 0doi: 10.1002/mrm.26190

Gruber S, Heckova E, Strasser B, Pova-zan M, Hangel GJ, Minarikova L, Trattnig S, Bogner W. Mapping an extended neurochemical profile at 3 and 7 T using accelerated high-resolution proton magnetic resonance spectroscopic imaging. Invest Radiol. 2017; 52:631–639. DOI: 10.1097/RLI.0000000000000379 [PubMed: 28459799]

Hangel G, Strasser B, Považan M, Gruber S, Chmelík M, Gajdošík M, Trattnig S, Bogner W. Lipid suppression via double inversion recovery with symmetric frequency sweep for robust 2D-GRAPPA-accelerated MRSI of the brain at 7 T. 2015; 28:1413–1425. DOI: 10.1002/nbm.3386

Hangel G, Strasser B, Považan M, Heckova E, Hingerl L, Boubela R, Gruber S, Trattnig S, Bogner W. Ultra-high resolution brain metabolite mapping at 7 T by short-TR Hadamard-encoded FID-MRSI. Neuroimage. 2016; doi: 10.1016/j.neuroimage.2016.10.043

Henning A, Fuchs A, Murdoch JB, Boesiger P. Slice-selective FID acquisition, localized by outer volume suppression (FIDLOVS) for 1H-MRSI of the human brain at 7 T with minimal signal loss. NMR Biomed. 2009; 22:683–696. DOI: 10.1002/nbm.1366 [PubMed: 19259944]

Hingerl L, Bogner W, Moser P, Pova-zan M, Hangel G, Heckova E, Gruber S, Trattnig S, Strasser B. Density-weighted concentric circle trajectories for high resolution brain magnetic resonance spectroscopic imaging at 7T. Magn Reson Med. 2018a; :79.doi: 10.1002/mrm.26987 [PubMed: 30014543]

Hingerl, L; Strasser, B; Moser, P; Považan, M; Hangel, G; He-ckov'a, E; Gruber, S; Trattnig, S; Bogner, W. Towards full-brain FID-MRSI at 7T with 3D concentric circle readout trajectories. International Society for Magnetic Resonance in Medicine; 26rd Annual Meeting, 2018; Paris p. 2018b. Abstract 5899

Jain S, Sima DM, Sanaei Nezhad F, Hangel G, Bogner W, Williams S, Van Huffel S, Maes F, Smeets D. Patch-based super-resolution of MR spectroscopic images: application to multiple sclerosis. Front Neurosci. 2017; 11doi: 10.3389/fnins.2017.00013

Li Y, Larson P, Chen AP, Lupo JM, Ozhinsky E, Kelley D, Chang SM, Nelson SJ. Short-echo three-dimensional H-1 MR spectroscopic imaging of patients with glioma at 7 tesla for characterization of differences in metabolite levels. J Magn Reson Imag. 2015; 41:1332–1341. DOI: 10.1002/jmri.24672

Libby CJ, Tran AN, Scott SE, Griguer C, Hjelmeland AB. The pro-tumorigenic effects of metabolic alterations in glioblastoma including brain tumor initiating cells. Biochim Biophys Acta Rev Canc. 2018; doi: 10.1016/j.bbcan.2018.01.004

Louis DN, Perry A, Reifenberger G, von Deimling A, Figarella-Branger D, Cavenee WK, Ohgaki H, Wiestler OD, Kleihues P, Ellison DW. The 2016 World Health organization classification of tumors of the central nervous system: a summary. Acta Neuropathol. 2016; 131:803–820. DOI: 10.1007/s00401-016-1545-1 [PubMed: 27157931]

Moser E, Stahlberg F, Ladd ME, Trattnig S. 7-T MR-from research to clinical applications? NMR Biomed. 2012; 25:695–716. DOI: 10.1002/nbm.1794 [PubMed: 22102481]

Nassirpour S, Chang P, Henning A. High and ultra-high resolution metabolite mapping of the human brain using 1H FID MRSI at 9.4T. Neuroimage. 2016; doi: 10.1016/j.neuroimage.2016.12.065

Ogg RJ, Kingsley PB, Taylor JS. WET, a T1- and B1-insensitive water-suppression method for in vivo localized 1H NMR spectroscopy. J Magn Reson B. 1994; 104:1–10. [PubMed: 8025810]

Považan M, Strasser B, Hangel G, Heckova E, Gruber S, Trattnig S, Bogner W. Simultaneous mapping of metabolites and individual macromolecular components via ultra-short acquisition delay 1 H MRSI in the brain at 7T. Magn Reson Med. 2018; 79:1231–1240. DOI: 10.1002/mrm.26778 [PubMed: 28643447]

Seltzer MJ, Bennett BD, Joshi AD, Gao P, Thomas AG, Ferraris DV, Tsukamoto T, Rojas CJ, Slusher BS, Rabinowitz JD, Dang CV, et al. Inhibition of glutaminase preferentially slows growth of glioma cells with mutant IDH1. Cancer Res. 2010; 70:8981–8987. DOI: 10.1158/0008-5472.CAN-10-1666 [PubMed: 21045145]

Senft C, Hattingen E, Pilatus U, Franz K, Schänzer A, Lanfermann H, Seifert V, Gasser T. Diagnostic value of proton magnetic resonance spectroscopy in the noninvasive grading of solid gliomas: comparison of maximum and mean choline values. Neurosurgery. 2009; 65:908–913. DOI: 10.1227/01.NEU.0000356982.82378.BA [PubMed: 19834403]

Stadlbauer A, Nimsky C, Buslei R, Pinker K, Gruber S, Hammen T, Buchfelder M, Ganslandt O. Proton magnetic resonance spectroscopic imaging in the border zone of gliomas: correlation of metabolic and histological changes at low tumor infiltration-initial results. Invest Radiol. 2007; 42:218–223. DOI: 10.1097/01.rli.0000255812.61435.67 [PubMed: 17351427]

Strasser B, Chmelik M, Robinson SD, Hangel G, Gruber S, Trattnig S, Bogner W. Coil combination of multichannel MRSI data at 7T: MUSICAL. NMR Biomed. 2013; 26:1796–1805. DOI: 10.1002/nbm.3019 [PubMed: 24038331]

Strasser B, Pova-zan M, Hangel G, Hingerl L, Chmelik M, Gruber S, Trattnig S, Bogner W. (2 + 1)D-CAIPIRINHA accelerated MR spectroscopic imaging of the brain at 7T. Magn Reson Med. 2017; 78:429–440. DOI: 10.1002/mrm.26386 [PubMed: 27548836]

Verburg N, Hoefnagels FWA, Barkhof F, Boellaard R, Goldman S, Guo J, Heimans JJ, Hoekstra OS, Jain R, Kinoshita M, Pouwels PJW, et al. Diagnostic accuracy of neuroimaging to delineate diffuse gliomas within the brain: a meta-analysis. Am J Neuroradiol. 2017; 38:1884–1891. DOI: 10.3174/ajnr.A5368 [PubMed: 28882867]

Wang Q, Zhang H, Zhang J, Wu C, Zhu W, Li F, Chen X, Xu B. The diagnostic performance of magnetic resonance spectroscopy in differentiating high-from low-grade glioma: a systematic review and meta-analysis. Eur Radiol. 2016; 26:2670–2684. DOI: 10.1007/s00330-015-4046-z [PubMed: 26471274]

Europe PMC Funders Author Manuscripts

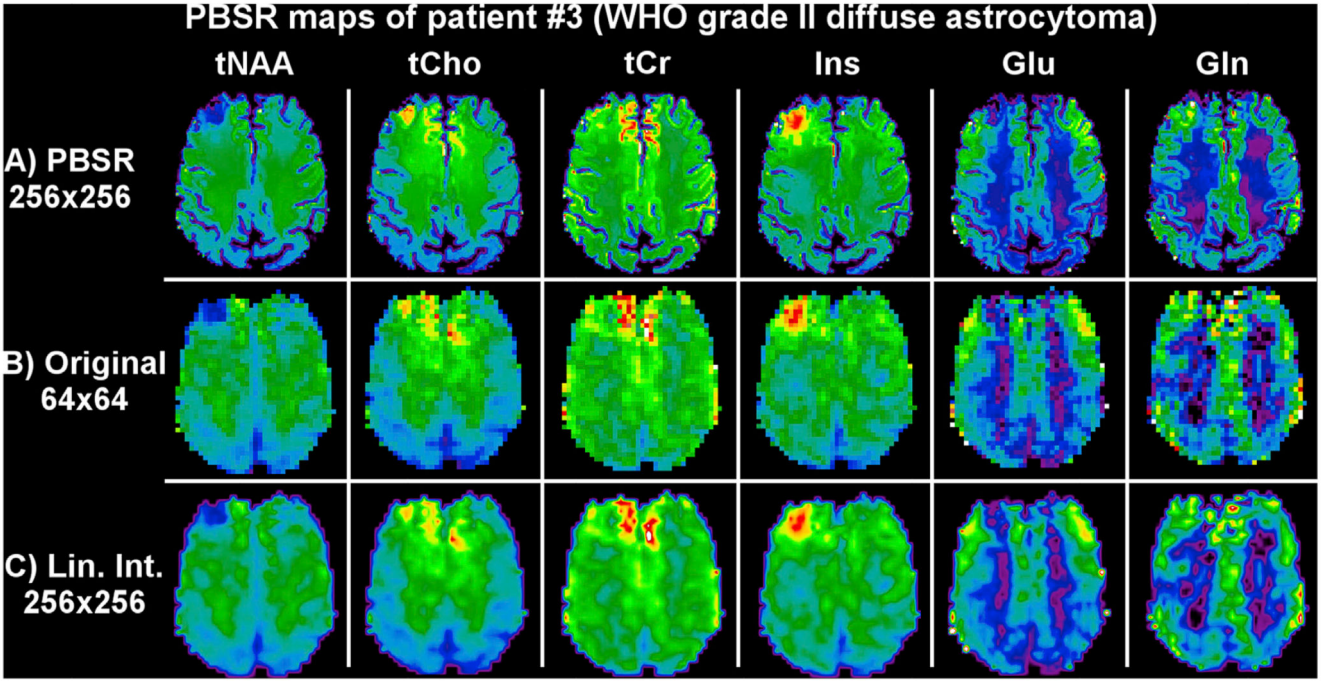

Fig. 1.

A comparison of the maps created by the application of PBSR (A) to the original maps (B) and standard linear interpolation (C). Both A and C increase the resolution by a factor of four, but only PBSR improves the information content. The resulting PBSR maps approach common MRI resolutions, eliminate CSF compartment effects, and improve the delineation of metabolic deviations within the glioma. The maps scale from low (purple) to high (red) relative values.

Europe PMC Funders Author Manuscripts

Europe PMC Funders Author Manuscripts

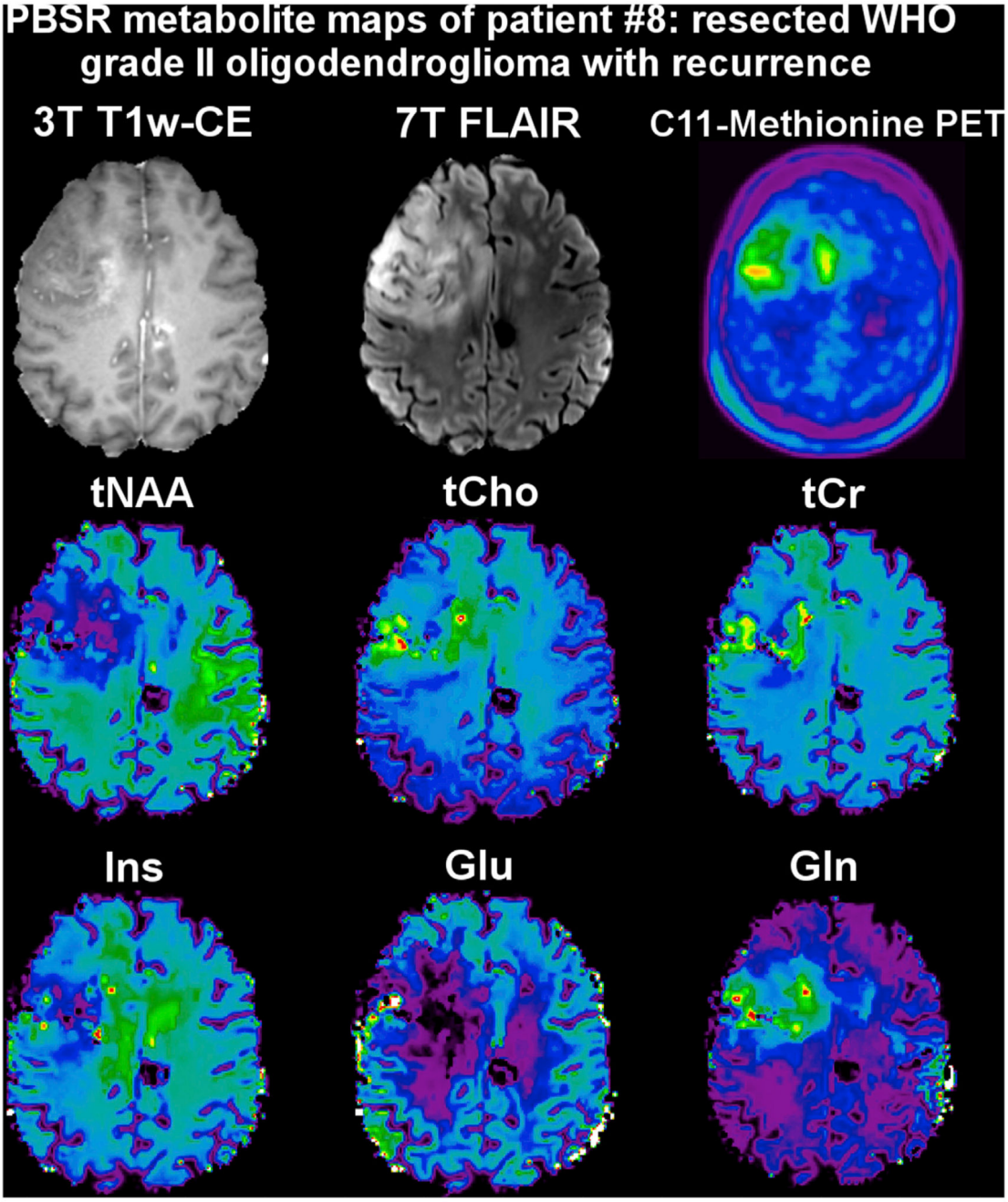

Fig. 2.

An overview of metabolite maps for a patient with a recurrence after resection of a WHO grade II oligodendroglioma compared to morphologic MRI and PET imaging. The metabolite maps show metabolic activities around the resection zone, including non-contrast-enhancing regions that correspond to the PET map, but offer more detail. Examples are Cho, which is a marker linked to tumor cell proliferation, and Gln, which consumption is increased in cancer cells. The Ins, tNAA and Gln maps suggest tumor activity in the other

hemisphere, in agreement with FLAIR-imaging. The maps scale from low (purple) to high (red) relative values.

Europe PMC Funders Author Manuscripts

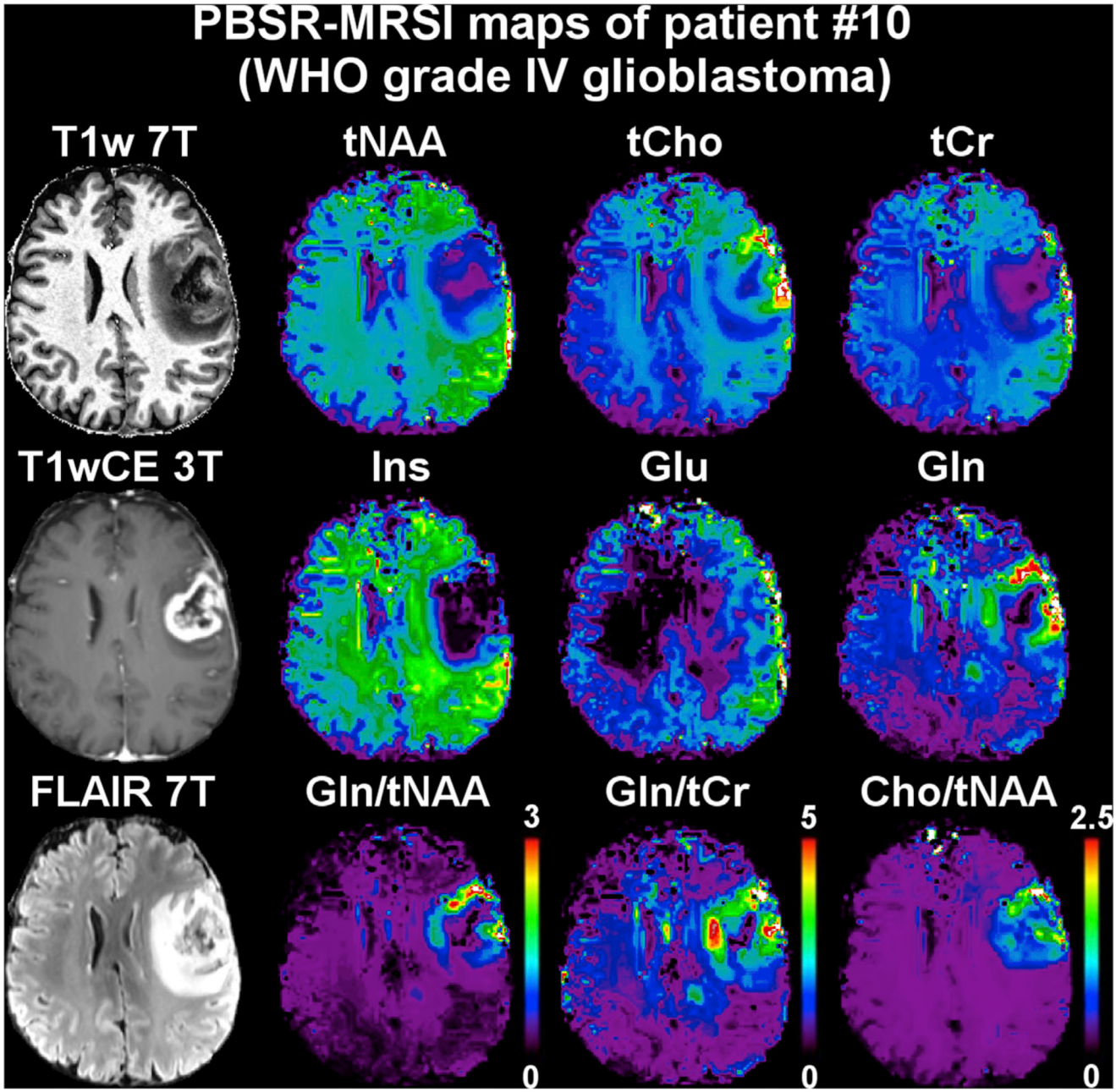

Fig. 3.

In this grade IV glioblastoma, the simultaneous acquisition of multiple metabolic contrasts showcases the ability of high resolution MRSI to resolve structural differences in tumors that correspond to morphologic imaging. Examples are increased Gln and tCho overlapping with contrast-enhanced T1w regions, tNAA and Ins drops and the hyper-intense FLAIR regions and a reduction of all metabolites in the presumably necrotic tumor center. The maps scale from low (purple) to high (red) relative values.

Europe PMC Funders Author Manuscripts

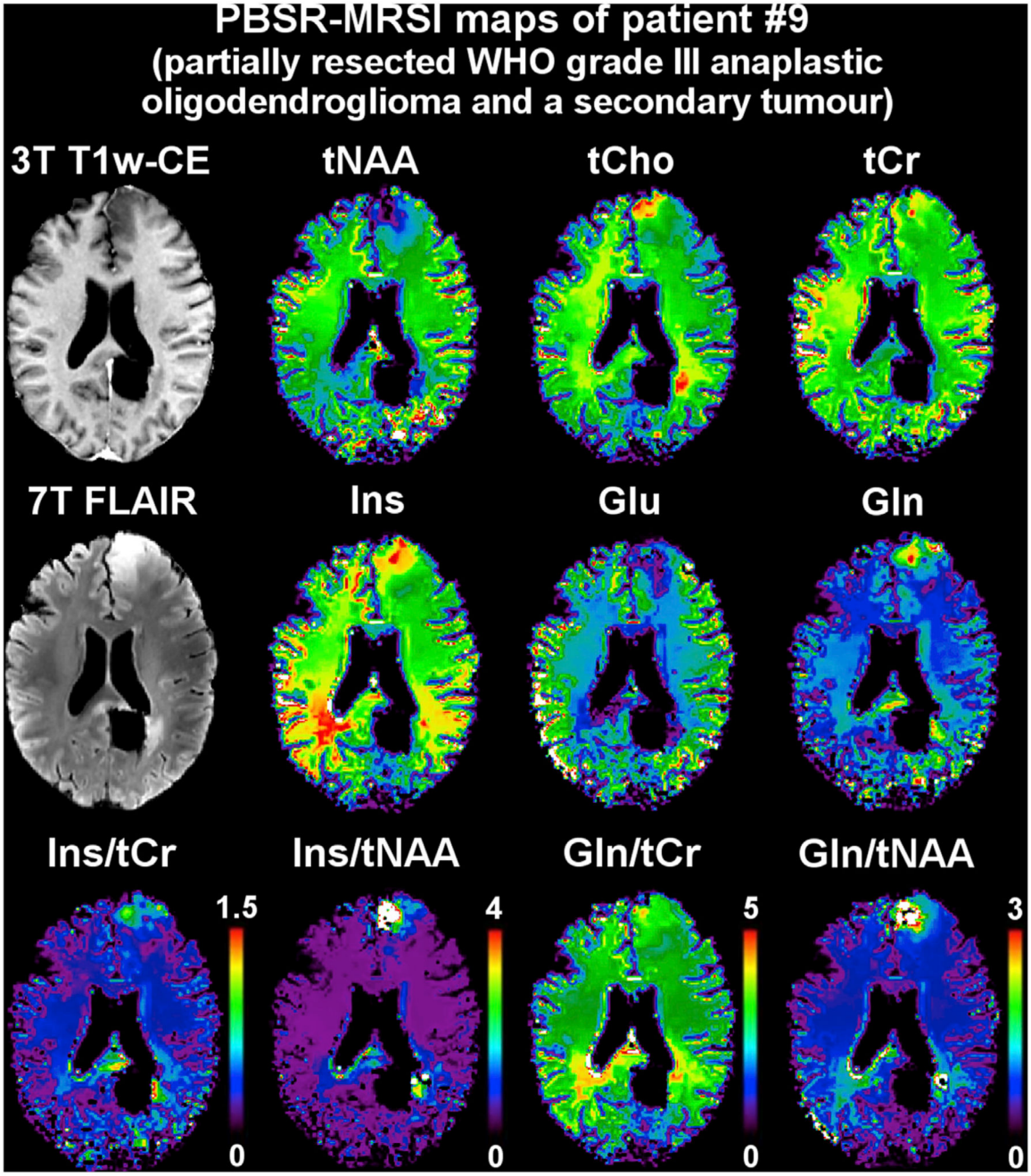

Fig. 4.

The metabolite maps of a patient with a partially resected grade III anaplastic oligodendroglioma and an additional left frontal lesion showcase the possibilities of high-resolution MRSI to resolve complex conditions. While the frontal lesion exhibits increases of Cho, Ins, and Gln, we also found metabolic activity in the periphery of the partially resected glioma, and contralaterally beyond the morphologically visible infiltration. This case is an example for the potential use of patient monitoring during treatment and after a resection. The maps scale from low (purple) to high (red) relative values.

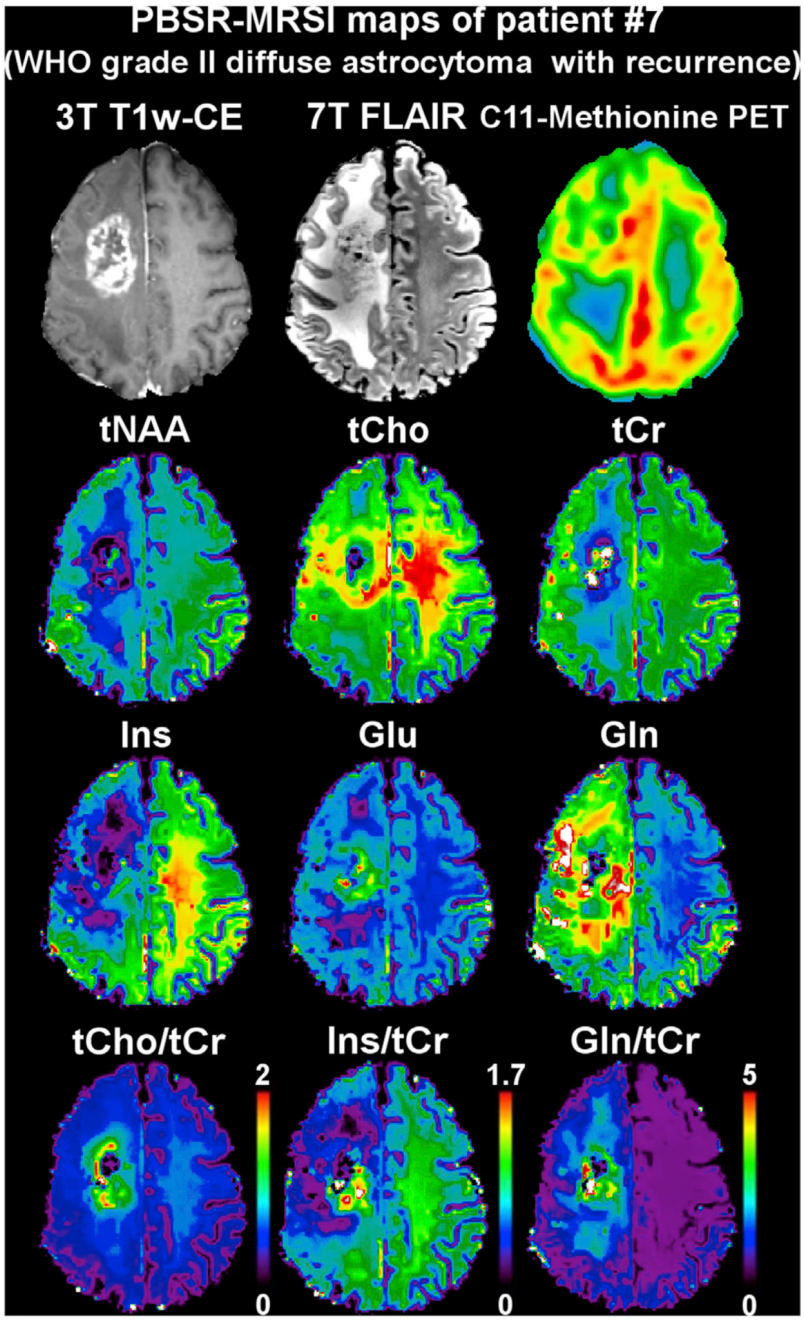

Fig. 5.

In this patient with an initially resected diffuse astrocytoma (WHO grade II) and recurrence, the metabolite and ratio maps show a differentiated behavior within various parts of the tumor beyond the contrast-enhancing regions. Most dominant is the ring-shaped increase of tCho around the resection zone overlapping with contrast enhancement and the spatially heterogeneous increase in Gln/reduction of Ins in the FLAIR-hyper-intense regions. In the center, the tNAA and tCr maps indicate quantification difficulties in the necrosis. The maps scale from low (purple) to high (red) relative values.

Europe PMC Funders Author Manuscripts

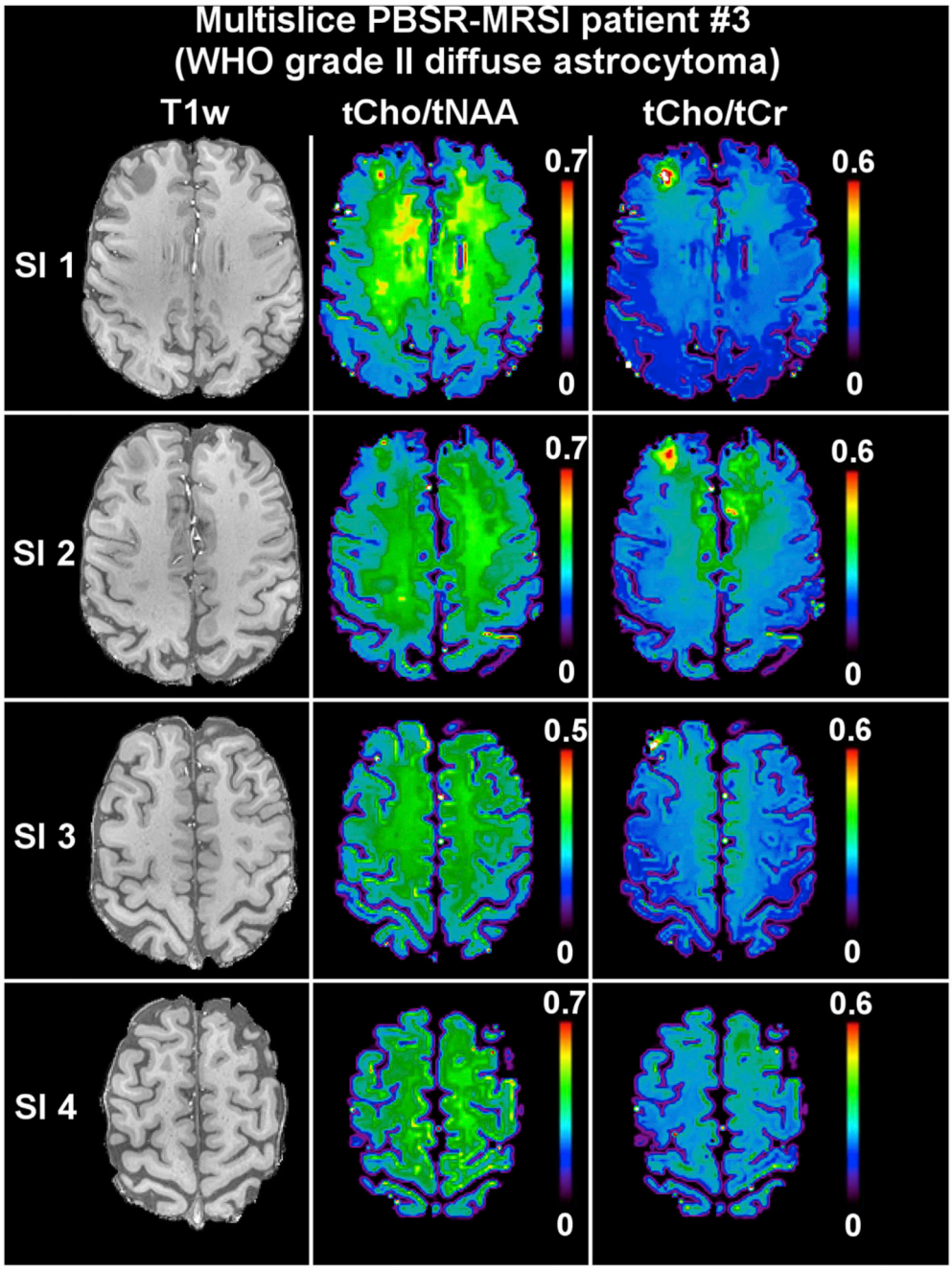

Fig. 6.

This multi-slice dataset shows the feasibility of PBSR for 3D-measurements for tCho/tNAA and tCho/tCr ratio maps. Despite the relatively small size of the grade II glioma and its proximity to the cranium, PBSR-MRSI allows to measure small subcortical gliomas. Albeit at longer measurement times of ~15min, multi-slice MRSI provides extended lesion coverage and/or the measurement of more distributed lesions.

Europe PMC Funders Author Manuscripts

Table 1

Diagnosis according to the WHO 2016 guidelines, IDH1-mutation status, 1p/19q-codeletion and trends of the metabolite behavior inside the solid glioma tissue for each patient. ↘ = predominantly decreasing; ↗ = predominantly increasing; ↗↘ = heterogeneous, both regions with an increase and a decrease. Over all patients, tNAA and Gln showed the clearest trends and tCr the most mixed behavior. The increase in Gln that is not observable on 3 T MRSI is particularly strong. Patients #7, #8 and #9 showed recurrence after a previous resection (on which the classification was based). In patient #9, a second tumor was present in the brain.

#	Histology	Grade	IDH1 mutant	1p/19q-codeletion	MRSI					
					tNAA	tCho	tCr	Ins	Glu	Gln
1	Oligodendroglioma	II	yes	yes	↘	↗	↘	↗	↘	↗
2	Anaplastic oligodendroglioma	III	yes	yes	↘	↗	↘	↗	↘	↗
3	Diffuse astrocytoma	II	yes	no	↘	↗	↘	↗	↘	↗
4	Anaplastic astrocytoma	III	yes	no	↘	↗	↘	↘	↘	↗
5	Diffuse astrocytoma	II	yes	no	↘	↗	↗	↗	↘	↗
6	Diffuse astrocytoma	II	yes	no	↘	↗	↗	↗	↘	↗
7	Diffuse astrocytoma	II	yes	no	↘	↗	↘	↘	↗	↗
8	Oligodendroglioma	II	yes	N/A	↘	↗	↗↘	↘	↘	↗
9	Anaplastic oligodendroglioma	III	yes	yes	↘	↗	↗	↗	↘	↗
10	Glioblastoma	IV	no	N/A	↘	↗↘	↘	↘	↗	↗

Europe PMC Funders Author Manuscripts

Table 2

Summary of 7 T MRI and MRSI sequence parameters. The PI-factor describes by how much the un-accelerated measurement time is divided.

Sequence	TR [ms]	TE [ms]	Scan time [min]	Matrix	Resolution [mm^3]	PI-factor
MPRAGE	3800	3.54	8	320 × 307 × 208	0.75 × 0.72 × 0.7	2
MP2RAGE	5000	4.13	8	320 × 320 × 224	0.75 × 0.75 × 0.75	3
FLAIR	9000	467	8	320 × 320 × 144	0.72 × 0.72 × 1	3
SWI	28	15	10	704 × 704 × 96	0.3 × 0.3 × 1.2	2
MRSI	600	1.3	12	64 × 64 × 1	3.4 × 3.4 × 8	3
MRSI	600	1.3	6	64 × 64 × 1	3.4 × 3.4 × 8	6
MRSI	600	1.3	15	64 × 64 × 4	3.4 × 3.4 × 8	9